Origin of the Giant Piezoelectric Properties in the [001] Domain Engineered Relaxor Single Crystals

Hichem DAMMAK[1*], Alexandra-Évelyne RENAULT[1,2], Philippe GAUCHER[1,2], Mai Pham THI[2] and Gilbert CALVARIN[1]

[1]*Laboratoire Structures, Propriétés et Modélisation des Solides UMR 8580 CNRS, École Centrale de Paris, Châtenay-Malabry 92295, France*
[2]*THALES Research & Technology France, Orsay Cedex 91404, France*

Relaxor single crystals PZN–9%PT have been cut and poled along [$\bar{1}$01] direction for which the spontaneous polarization $\boldsymbol{P}_s$ is approximately parallel to the poling field $\boldsymbol{E}_p$. The piezoelectric matrix of the monoclinic single-domain (1M state) has been determined, in the approximation of an orthorhombic symmetry. The shear mode (15) along [101], gives the highest electromechanical coupling factor k_{15} (>80%) and the largest piezoelectric coefficient d_{15} (~3200 pC/N). The properties of the disoriented 1M state have been calculated from a change of axes. The maximum of $d_{33}^{\theta\varphi}$ is obtained along a direction close to [001]. This is due to the very large value of d_{15} compared to d_{33} in the basic 1M state. On the other hand the transverse piezoelectric coefficient along [uv0] for the [001] disoriented $\boldsymbol{P}_s$ single domain presents a strong anisotropy. Finally, in the [001] domain engineered configuration, an important extrinsic contribution of the domain coexistence is evidenced by comparing calculated and measured coefficients.   [DOI: 10.1143/JJAP.42.dummy]

KEYWORDS: PZN–PT, piezoelectric matrix, single-domain and multidomain, shear mode

1. Introduction

Piezoelectric single crystals based on perovskite lead oxides, like Pb(Mg$_{1/3}$Nb$_{2/3}$)O$_3$–PbTiO$_3$ (PMN–PT) or Pb(Zn$_{1/3}$Nb$_{2/3}$)O$_3$–PbTiO$_3$ (PZN–PT), are presently subject of a lot of research because of their very high field induced static strain[1] (greater than 1%) and of their very high electromechanical coupling coefficients in dynamic use, especially for the length-extensional modes[2-5] ($k_{33} \sim 93\%$ and $k_{31} \sim 80\%$). Despite the difficulty to synthesize them with a good homogeneity and a reasonable size, they are expected to replace PZT ceramics [Pb(Zr$_{1-x}$Ti$_x$)O$_3$] in some applications like acoustic ranging and imaging, steady state actuators, active vibration control, etc....

The origin of this giant piezoelectric effect is not completely understood, because of the complexity of the (E, T) phase diagram which depend on the poling protocol used, and the few studies on the domain structure related to these different phases. In fact, the electromechanical properties of these compounds depend on several parameters:

– Chemical composition x in PZN–x%PT having a major effect on the phase transitions sequence.[2]

– Poling direction and crystallographic orientation: most of the studies are made using pseudo-cubic [001][6] oriented crystals, which give the best performances, at least in longitudinal (33) mode and transverse (31) mode along [100].[1,2]

– Poling protocol:[5,7,8] it is an important parameter of the "sample history". The constant field and temperature method (CF poling method) is the most commonly used, but other methods are also possible: cooling from above the Curie temperature T_C to room temperature (RT), under an electric field (FC or field cooling method), or progressive increase of the field at a constant temperature (IF method).

In the case of PZN–9%PT, recent results show that the structure at RT is not the mixture of rhombohedral and tetragonal phases as previously reported[2] but is a mixture of monoclinic (M) and tetragonal (T) phases.[8,10] The coex-istence of two phases is due to the wide hysteresis which characterizes the M ↔ T transition when the temperature is cycled: M → T and T → M transitions occurs at ~350 and ~290 K respectively.[5,9] On the other hand, crystals recover mainly the M phase at RT, after cooling and heating cycle.[5,9,10] We have shown recently[9] that PZN–9%PT poled single crystals are monoclinic at RT and that optical observations, dielectric and high resolution X-ray measurements show that crystals can adopt different monoclinic domain structures according to the direction of the poling field. A monoclinic quasi-single domain (1M) was obtained for the first time by poling the crystal along the pseudo-cubic [10$\bar{1}$] direction. When crystals are poled along [001], a more complex monoclinic domain state is obtained, because the polar axis makes an angle of about 45° with the poling direction. Two different domain states were obtained: a 2-domain state (2M) with a macroscopic 2mm symmetry and a 4-domain state (4M) with a macroscopic 4mm symmetry.[9]

The aim of this paper is to determine the complete intrinsic piezoelectric matrix of ($\bar{1}$01) cut PZN–9%PT single crystals, i.e., in the 1M state. The experimental values of piezoelectric constants d_{31} and d_{33} of (001) cut PZN–9%PT single crystals in the engineered domain configuration are then compared to those calculated by using the intrinsic piezoelectric matrix of the 1M state.

2. Experimental Methods

Crystals were grown by the flux method as described previously by Renault *et al.*[8,9] They were cut and polished with different orientations: [101]/[010]/[$\bar{1}$01] (A), [100]/[010]/[001] (B) and [110]/[$\bar{1}$10]/[001] (C), in order to obtain side-plated and end-plated bars with typical sizes: $\ell = $ 3–5 mm, $w = $ 1–1.5 mm and $t = $ 1–1.5 mm. Thin films of Cr/Au electrodes (~100 nm Au) were sputtered on the ($\bar{1}$01) or (001) faces.

Bars A were poled by IF method at RT along one of the two equivalent ⟨101⟩ directions in order to obtain the 1M state. Taking into account the very small monoclinic distortion of the M phase, the elasto-piezo-dielectric matrix could be similar to that of the O phase ($B2mm$), like KNbO$_3$ single crystals[11,12] at RT, for which the matrix is as below:

*E-mail address: dammak@spms.ecp.fr

$$\begin{pmatrix}
S_{11}^{E} & S_{12}^{E} & S_{13}^{E} & & & & & & d_{31} \\
S_{21}^{E} & S_{22}^{E} & S_{23}^{E} & & & & & & d_{32} \\
S_{31}^{E} & S_{32}^{E} & S_{33}^{E} & & & & & & d_{33} \\
& & & S_{44}^{E} & & & & d_{24} & \\
& & & & S_{55}^{E} & & d_{15} & & \\
& & & & & S_{66}^{E} & & & \\
& & & & d_{15} & & \epsilon_{11}^{T} & & \\
& & & d_{24} & & & & \epsilon_{22}^{T} & \\
d_{31} & d_{32} & d_{33} & & & & & & \epsilon_{33}^{T}
\end{pmatrix}$$

where the X (1), Y (2) and Z (3) axes correspond to the [101], [010] and [$\bar{1}$01] directions, respectively. For measuring the shear coefficient d_{15} or d_{24}, the electrodes used for poling were removed and new electrodes were sputtered on the smallest faces perpendicular to the first ones, allowing to have the larger dimension for propagation of the acoustic waves in the shear mode (leading to the lowest resonance frequency).

Multidomain states were obtained with bars B and C by applying a poling field along [001], varying between 100 and 400 kV/m, in FC run with a cooling rate equal to 2 K/min. Crystals were cooled down from 470 K to ~250 K then heated up to RT, in order to recover completely the monoclinic phase and to avoid the tetragonal phase.

To describe the piezoelectric properties of the poled multidomain state, we were brought to define a special notation: $d_{31}^{[001]/[100]}$ and $d_{31}^{[001]/[110]}$ mean the transverse piezoelectric coefficients for which the ac electric field $\boldsymbol{E}_a$ is applied along [001] and the acoustic wave propagation direction is parallel to [100] and [110], respectively. The longitudinal coefficient is noted simply $d_{33}^{[001]}$ because $\boldsymbol{E}_a$ and the propagation direction are parallel.

The dielectric permittivity was measured at 10 kHz, 0.5 V$_{rms}$ using a HP 4192A impedance analyzer. The electromechanical coupling factors $k_{i\alpha}$, the piezoelectric coefficients $d_{i\alpha}$ and the elastic compliances $s_{\alpha\beta}^{E}$ were derived from the IRE method using the impedance spectra near resonance. Depending on the distances of the wave propagation, the resonance frequencies were observed between 100 and 700 kHz.

3. Experimental Derivation of the Elasto-Piezo-Dielectric Matrix for the 1M State

Figure 1(a) shows that, after poling along [$\bar{1}$01], the spontaneous polarization $\boldsymbol{P}_s$ is close to the saturated polarization. On the other hand, the relative dielectric permittivity ϵ_{33}^{T} and the piezoelectric coefficient d_{31} follow the normal

Fig. 1. (a) Displacement current density, measured during the polarization of crystal A in IF run along [$\bar{1}$01]. The polarization is derived by integration of this current density. (b) Variation of the permittivity and of the piezoelectric coefficient as a function of the dc field in the previously poled crystal A.

linear decrease when the dc electric field is applied along [$\bar{1}$01] in the same sense as the poling field [Fig. 1(b)]. These results show, as we previously reported,[9] that the 1M state is stable, without partial depoling, when the field is removed.

The measured constants are listed in Table I and compared to those of the O phase of KNbO$_3$ single crystals.[13] As the IRE method does not allow to determine the sign of $d_{i\alpha}$, we attributed the same signs as for KNbO$_3$. Indeed, by comparing the lattice parameter of the cubic cell a_c with the ones of the ferroelectric O cell a_0, b_0 and c_0 [Fig. 2(a)], one can note that the positive signs of d_{31} and d_{33} are coherent with the increase of the lattice distances along [101] ($a_0 > \sqrt{2}a_c$) and [$\bar{1}$01] ($c_0 > \sqrt{2}a_c$), respectively (Table I). In other words, the creation of a polar moment along [$\bar{1}$01] leads to an elongation of the lattice parameters in the (010) plane and a contraction along the [010] direction.

Table I. Components of the dielectric ε^{T}, elastic s^{E} (10^{-12} m^2/N), piezoelectric d (10^{-12} C/N) matrixes and of the anisotropic distortion of the ferroelectric cell, for PZN–9%PT and KNbO$_3$ single crystals in their 1M and 1O states respectively.

		PZN–9%PT (1M)				KNbO$_3$ (1O)[13]			
$\varepsilon_{11}, \varepsilon_{22}, \varepsilon_{33}$		9000	21000	800		150	945	44	
$d_{31}, d_{32}, d_{33}, d_{24}, d_{15}$	(pC/N)	120	−270	250	950	3200	9.8	−19.5	29.3	160	214
$s_{11}, s_{22}, s_{33}, s_{44}, s_{55}$	(pm^2/N)	11	25	18	13	187	5.4	5.1	7	13.5	40
$k_{31}, k_{32}, k_{33}, k_{24}, k_{15}$	(%)	45	62	60	60	80	22,	44	56	48	90
$\frac{a_0}{\sqrt{2}a_c}-1, \frac{b_0}{a_c}-1, \frac{c_0}{\sqrt{2}a_c}-1$	(%)	9×10^{-2}	-64×10^{-2}	40×10^{-2}		30×10^{-2}	-104×10^{-2}	76×10^{-2}		

4. Calculation of the Piezoelectric Components for a [001] Oriented Crystal in the 1M State

The calculation method of the components of the piezo-electric matrix for a [001] oriented crystal in the 1M state (polarization off-axis as regards to the field), from the data of a [$\bar{1}$01] oriented crystal (polarization in-axis), is based on the transformation of axes by using the spherical coordinate system [Fig. 2(b)]. The transformation matrix is given as following:

$$\begin{pmatrix} \cos\chi\cos\theta\cos\varphi - \sin\chi\sin\varphi & \cos\chi\cos\theta\sin\varphi + \sin\chi\cos\varphi & -\cos\chi\sin\theta \\ -\sin\chi\cos\theta\cos\varphi - \cos\chi\sin\varphi & -\sin\chi\cos\theta\sin\varphi + \cos\chi\cos\varphi & \sin\chi\sin\theta \\ \sin\theta\cos\varphi & \sin\theta\sin\varphi & \cos\theta \end{pmatrix}.$$

In the new reference, calculated $d_{i\alpha}^{\theta\varphi\chi}$ depends on angles θ, φ and χ. The component $d_{33}^{\theta\varphi\chi}$ is χ independent:

$$\begin{aligned} d_{33}^{\theta\varphi} = \cos^3\theta d_{33} &+ \cos\theta\sin^2\theta\{\cos^2\varphi(d_{31} + d_{15}) \\ &+ \sin^2\varphi(d_{32} + d_{24})\} \end{aligned} \quad (1)$$

Figure 3(a) shows its variation as a function of θ, in the (010) plane ($\perp$[010]), i.e. $\varphi = 0°$. A maximum value is obtained for $\theta_{\max} = 53.2°$; this value is much higher than the one obtained in the [$\bar{1}$01] orientation, i.e., for $\theta = 0°$: $d_{33}^{\theta_{\max},\varphi=0°}/d_{33} \sim 5$. Let us remark that the $\theta_{\max}$ angle is close to that between [001] and [$\bar{1}$01] ($\theta = \pm45°$, neglecting the orthorhombic distortion). As expected, $d_{33}^{\theta\varphi}$ tends towards zero near the [101] direction which is perpendicular to $\boldsymbol{P}_s$.

The large enhancement of $d_{33}^{\theta\varphi}$ around $\theta_{\max}$ is due to the much larger value of d_{15} compared to d_{33}. Indeed, when $d_{15} \gg d_{33}$ and $d_{15} \gg d_{31}$ in relation (1), $\theta_{\max}$ tends towards 57.4°, i.e., $\cos(\theta_{\max}) = 1/\sqrt{3}$, and $d_{33}^{\theta_{\max},\varphi=0}$ tends to $2d_{15}/(3\sqrt{3})$. In other words, the piezoelectric strain comes not only from the elongation of the polar vector, but mainly from its tilting under $\boldsymbol{E}_a$.
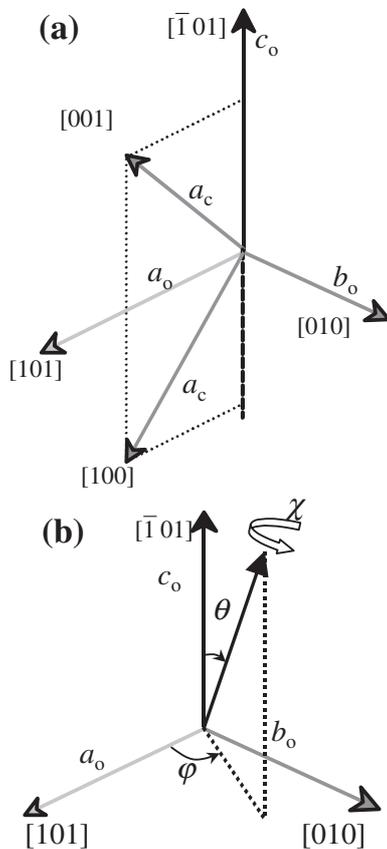
Fig. 2. (a) Pseudocubic and orthorhombic crystallographic axes and relative orientations of [$\bar{1}$01], [101], [010], [100] and [001], and (b) orthorhombic unit cell and spherical coordinates related to it.
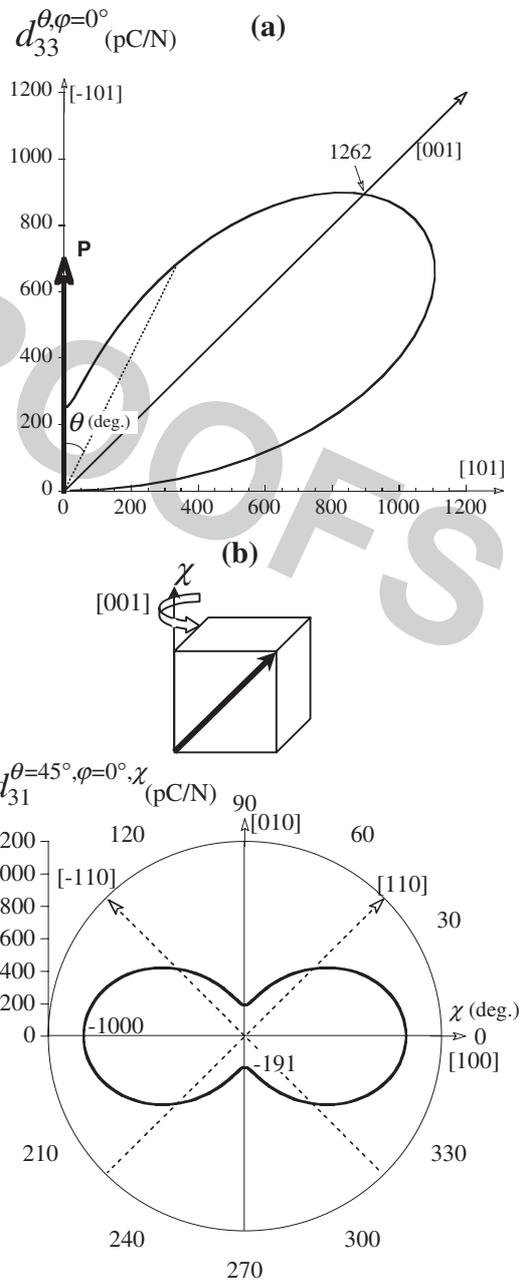
Fig. 3. Angular dependence of calculated piezoelectric coefficients of PZN–9%PT single crystal in the length-extensional mode: (a) $d_{33}^{\theta,\varphi=0}(\theta)$ and (b) $d_{31}^{\theta=45,\varphi=0,\chi}(\chi)$ curves in the polar coordinate system.

Figure 3(b) shows the variation, as a function of χ, of the transverse piezoelectric coefficient in the (001) plane ($\perp$[001]), i.e., $\theta = 45°$ and $\varphi = 0$. The maximum value of $d_{31}^{\theta=45°,\varphi=0,\chi}(= d_{31}^{[001]/[uv0]})$ is obtained along [100] which belongs to the plane defined by [001] and $\boldsymbol{P}_s$ [Fig. 3(b)]. $d_{31}^{[001]/[uv0]}$ is minimum along [010] which is perpendicular to $\boldsymbol{P}_s$.

In these latter calculations we consider the [001] oriented crystal in the 1M state, i.e. constituted by only one domain. When crystals are poled along [001], four equivalent domain families can coexist. To calculate the piezoelectric matrix of this structure, the orientation relationships between these domains should be considered. We denote the four equivalent domain families as M_1, M_2, M_3 and M_4; they correspond to the orientation angles $(\theta, \varphi, \chi) = (45, 0, 0)$, $(-45, 0, 0)$, $(45, 0, 90)$ and $(-45, 0, 90)$, respectively [Fig. 4(a)]. Using the transformation matrix, the piezoelectric matrix (pC/N) of

(a)

(b)

(c)

each domain family is as following:

$$(d_{i\alpha}^{M_1}) = \begin{pmatrix} -1262 & 191 & 1000 & 0 & 92 & 0 \\ 0 & 0 & 0 & 672 & 0 & -672 \\ -1000 & -191 & 1262 & 0 & -92 & 0 \end{pmatrix},$$

$$(d_{i\alpha}^{M_2}) = \begin{pmatrix} 1262 & -191 & -1000 & 0 & 92 & 0 \\ 0 & 0 & 0 & 672 & 0 & 672 \\ -1000 & -191 & 1262 & 0 & 92 & 0 \end{pmatrix},$$

$$(d_{i\alpha}^{M_3}) = \begin{pmatrix} 0 & 0 & 0 & 0 & 672 & 672 \\ -191 & 1262 & -1000 & 92 & 0 & 0 \\ -191 & -1000 & 1262 & 92 & 0 & 0 \end{pmatrix},$$

$$(d_{i\alpha}^{M_4}) = \begin{pmatrix} 0 & 0 & 0 & 0 & 672 & -672 \\ 191 & -1262 & 1000 & 92 & 0 & 0 \\ -191 & -1000 & 1262 & -92 & 0 & 0 \end{pmatrix}.$$

One can note, in particular, the strong anisotropy of the transverse and shear piezoelectric coefficients. For example, in M_1 type domains: $d_{31}^{M_1} \approx 5d_{32}^{M_1}$ and $d_{24}^{M_1} \approx 7d_{15}^{M_1}$. The calculation of the piezoelectric coefficients of the multidomain state could be obtained *a priori* by a linear combination of these matrix:

$$(d_{i\alpha}^{4M}) = x_1(d_{i\alpha}^{M_1}) + x_2(d_{i\alpha}^{M_2}) + x_3(d_{i\alpha}^{M_3}) + x_4(d_{i\alpha}^{M_4}). \quad (2)$$

However, this calculation needs the knowledge of the relative rate of each domain family in the crystal. The determination of this rate is not easy and moreover it can change from crystal to another.

5. The Effect of Domain Coexistence on the Piezoelectric Properties

Table II gives the measured and calculated values of the piezoelectric coefficients. Regarding measured piezoelectric coefficients, let us note that the values of $d_{31}^{[001]/[100]}$ varies strongly from -1840 to -910 pC/N when the poling field, during FC run, increases; on the other hand, $d_{31}^{[001]/[110]}$ varies little (-1100 to -900 pC/N). This different behavior can be explained by the strong anisotropy of $d_{31}^{[001]/[uv0]}$ [Fig. 3(b)]. Indeed, for a given domain family, $d_{31}^{[001]/[110]}$ is equal to $d_{31}^{[001]/[\bar{1}10]}$, while $d_{31}^{[001]/[100]}$ and $d_{31}^{[001]/[0\bar{1}0]}$ are very different. For a [001] poled crystal, with propagation modes along [100] (resp. [010]), domain families M_1 and M_2 (resp. M_3 and M_4) lead to -1000 pC/N while domain families M_3 and M_4 (resp. M_1 and M_2) lead to -191 pC/N. So the effective $d_{31}^{[001]/[100]}$ depends on the domain structure and is expected to vary between -191 and -1000 pC/N.
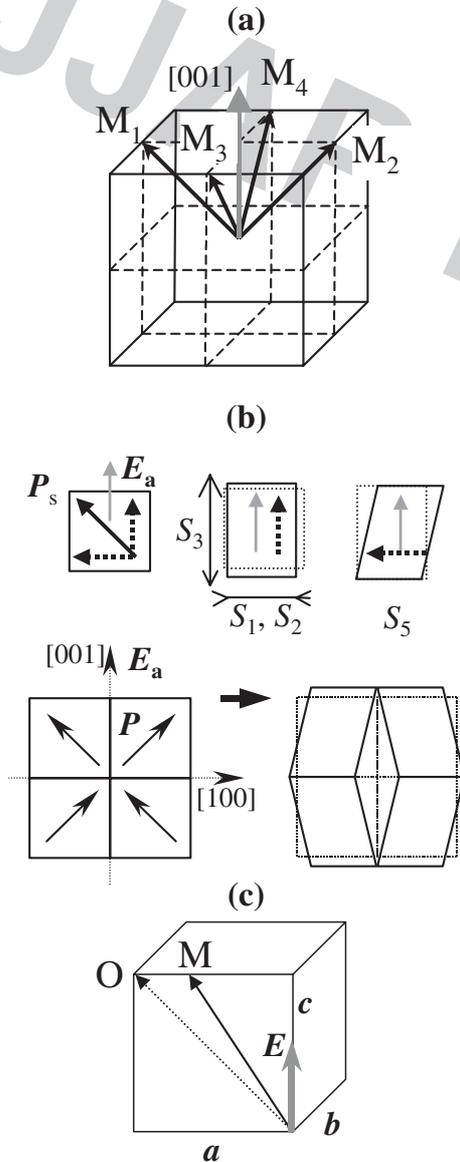
Fig. 4. (a) Schematic representation of the four domains in the 4M state. (b) Free piezoelectric strain of a single domain and schematic representation of the 2M state showing the shear strain of the two opposite (twin) domains such as M_1 and M_2 or M_3 and M_4. (c) Monoclinic distortion of the O phase in single crystals poled along [001].

Table II. Measured and calculated piezoelectric $d_{i\alpha}$ (10^{-12} C/N) components of [001] oriented PZN–9%PT and KNBO$_3$ single crystals.

	PZN–9%PT		KNBO$_3$[12]	
	measured	calculated	measured	calculated
$\varepsilon_{33}^{[001]}$	4900–5300	4900		
$d_{33}^{[001]}$	2500–2700	1262	90–95	87.2
$-d_{31}^{[001]/[110]}$	900–1100	596		
$-d_{31}^{[001]/[100]}$	910–1840	191 or 1000		

On the other hand, one can note that the measured values of $d_{33}^{[001]}$ and $d_{31}^{[001]/[110]}$, as well as that of $d_{31}^{[001]/[100]}$, are more than twice the calculated ones. So, the effective piezoelectric coefficients are still larger than that expected by assuming only the effect of polarization (P_s) orientation as regards to the direction of applied electric field E_a. This orientation is already almost optimum (45°). To explain this difference between measured and calculated values, two effects should to be considered:

1. Induced dynamic stresses between adjacent domains: this effect is related to the coexistence of domain families in the case of macroscopic [001] poling. The difference between a single domain with P_s tilted 45° away from E_a (M$_1$, M$_2$, M$_3$ or M$_4$), and a macroscopic real multidomain state is that, in the second case, the induced shear strain of two opposite domains are counteracting. For twin-domains M$_1$ and M$_2$ (or M$_3$ and M$_4$) for example, the induced longitudinal and transverse strains $(S_3 = d_{33}^{M_1}E_3,\ S_1 = d_{31}^{M_1}E_3,\ S_2 = d_{32}^{M_1}E_3)$ are the same for the domain families M$_1$ and M$_2$, while the induced shear strains are opposite $(S_5 = d_{35}^{M_1}E_3,\ d_{35}^{M_1} = -d_{35}^{M_2})$ [Fig. 4(b)]. When applying E_a along the [001] poling direction, the two P_s vectors tend to tilt towards the direction of this field, but the coexistence of domain families, i.e., domain walls, prevents the shear of both domains, and leads to an additional shear stress component T_5. When the four domain families coexist with a 3D network in the crystal, additional internal stresses have to be considered due to the anisotropy of $d_{31}^{[001]/[uv0]}$. These lattice extrinsic stresses, induced indirectly by E_a, contribute then to additional longitudinal and transverse distortions, increasing the effective $d_{33}^{[001]}$ and $d_{31}^{[001]/[uv0]}$ coefficients. In that case, the calculation of piezoelectric coefficients, by averaging the contribution of each domain family, as shown in relation (2), is not adapted, and the compliance $s_{\alpha\beta}$, via the domain structure, should be also taken into account: $d_{i\alpha}^{4M} = f\,(d_{j\beta},\ s_{\alpha\beta},$ domain structure). This explanation remains to be quantified, from an estimation of the contribution of the internal stresses in some modeled domain structures.

2. Static monoclinic distortion due to off-axis poling: after poling along [001], the monoclinic distortion of the ferroelectric phase of PZN–9%PT increases.[9] The polar moment is tilted in the (010) plane to approach [001][14] [Fig. 4(c)]. Taking into account the important monoclinic distortion in the poled multidomain states, the approximation, as considered above, within the framework of the O symmetry, is not valid any more; in that case it is thus necessary to consider 10 independent piezoelectric components to describe the piezoelectric matrix of the M phase.

6. Comparison between Simple and Complex Perovskites

In the single-domain state of the both compounds PZN–9%PT and KNbO$_3$, the shear mode (15) gives the highest electromechanical coupling factor k_{15} and the largest piezoelectric coefficient d_{15} (Table I). However, there are two important differences between these two compounds. First, the components of the elasto-piezo-dielectric matrix are more important for PZN–9%PT than for KNbO$_3$ showing that the first material is more sensitive to the stress and to the electric field. Secondly, the ratios $\varepsilon_{11}/\varepsilon_{33}$, d_{15}/d_{33} and s_{55}/s_{33} are larger for PZN–9%PT (resp. ∼11, 13 and 10) than for KNbO$_3$ (resp. ∼3, 7 and 6) meaning that for the first crystal P_s changes its direction, by tilting in the (010) plane, more easily than its magnitude. These remarks concerning the intrinsic properties observed on a single domain could be generalized for other complex or simple perovskites. Indeed, Zhang *et al.*[15] show that for the rhombohedral phase of PZN–4.5%PT and PZN–8%PT crystals poled along [111], k_{15} is equal to 90 and 93% respectively, and d_{15} is equal to 2500 and ∼5500 pC/N respectively. Using the value of d_{33} determined by Liu *et al.*,[16] the ratio d_{15}/d_{33} is then of about 20 for PZN–4.5%PT. In a simple perovskite like BaTiO$_3$ crystals in the tetragonal phase, the values[17] of d_{15} and d_{15}/d_{33} are equal to 392 pC/N and ∼5 respectively and they remains lower than those of PZN–PT compounds.

In the multidomain state, the effect of domain coexistence should be normally observed for [001] poled crystals whatever the domain symmetry is: orthorhombic (O), rhombohedral (R) or monoclinic (M). However, the enhancement of $d_{33}^{[001]}$ by the induced internal stress effect is not so important for simple perovskites like KNbO$_3$, it is only about 10%[12] (Table II). On the other hand, the difference between calculated and measured values is very important for PZN–9%PT. This different behavior can be related to the differences in the structural and mechanical properties of these two compounds:

1. The ferroelastic distortion of the polar cell is more important for KNbO$_3$ (∼1%) than for PZN–9%PT (∼0.6%) (Table I). So, the local strain S between 90°-domains is twice lower for PZN–PT.

2. The compliance s is three times lower for KNbO$_3$ than for PZN–9%PT (Table I). So, for the same strain of a single domain, the stress T is three times lower for PZN–PT.

Consequently, for a given multidomain state, the static elastic energy is about twelve times lower for PZN–PT. This leads, for KNbO$_3$, to the formation of domains with sizes comparable to that of the crystal[12] and a low density of domain walls, while a multidomain state, with a more important density of domain walls, can be stabilized in the case of PZN–PT. This explains the small sizes ($<100\,\mu$m)[9,18] and the 3D network of domains in PZN–9%PT single crystals. In this compound, domains interact much more strongly and the extrinsic contribution, due to the coexistence of domains, is important.

7. Conclusion

Relaxor single crystals, cut along the [001] direction, are known to have a local spontaneous polarization P_s which is "off-axis" as regard to the poling electric field E_p. The following points were clarified in this paper:

1. The complete piezoelectric matrix of the single-domain state with in-axis polarization was measured using a [$\bar{1}$01] oriented PZN–PT crystal, assuming an orthorhombic symmetry.

2. The piezoelectric matrix was calculated, for an arbitrary disorientation of P_s with respect to E_a, using a linear matrix transformation in a spherical coordinate system

with angles θ, φ and χ. It was shown that the maximum value of $d_{31}^{\theta\varphi}$ corresponds to a direction close to [001]. The enhancement of $d_{33}^{\theta\varphi}$ was explained by the much larger value of d_{15} with respect to d_{33} in the basic domain structure described in §3. The longitudinal strain in off-axis domains is so mainly related to a tilting of $\boldsymbol{P}_s$ rather than to its elongation.

3. A strong anisotropy was found for the transverse piezoelectric coefficient $d_{31}^{[001]/[uv0]}$ in the (001) plane, i.e., $\theta = 45°$ and $\varphi = 0°$. This coefficient is maximum when the propagation wave vector is in the plane defined by $\boldsymbol{P}_s$ and $\boldsymbol{E}_a$ and minimum in the perpendicular direction.

4. The measured coefficient $d_{33}^{[001]}$ is about twice larger in [001] engineered domain crystals than the one calculated in the [001] disoriented single domain. To explain this, two hypothesis are suggested:

   a. A contribution of internal dynamic stresses, due to the coexistence of 4 domain families and to the anisotropy of piezoelectric coefficients in each domain family has to be added to the individual contribution of each domain family.

   b. The poling in a direction different to that of $\boldsymbol{P}_s$ increases the monoclinic distortion and the ortho-rhombic approximation is no more valid.

5. The strong dispersion of experimental values of $d_{31}^{[001]/[100]}$ coefficient in the [001] multidomain states, can be explained by its strong dependence with respect to the propagation direction ([010] or [100]) for each domain family and to the domain microstructure which is uncontrolled at the macroscopic scale.

6. The comparison between a simple perovskite, like KNbO$_3$, and a complex disordered one, like PZN–PT, leads to the following remarks:

   a. In the single-domain state, the ratio d_{15}/d_{33} is much larger in PZN–PT than in KNbO$_3$, probably because of the proximity of a phase transition in the first case.[19]

   b. In the multidomain state, the internal static stresses, due to the coexistence of domain families, is about 10 times smaller in KNbO$_3$ than in PZN–PT, leading to larger domain sizes for the first compound and a large number of small domains for the second one. So, the influence of domain walls in the engineered domain structures, that we can call "extrinsic contribution", is negligible in KNbO$_3$ and important in PZN–PT.

All these features make evidence that the prediction of the complete elasto-piezo-dielectric matrix of the engineered domain relaxor single crystals will need a complete and quantitative description of the domain structure.

1) S.-E. Park and T. R. Shrout: J. Appl. Phys. **82** (1997) 1804.
2) J. Kuwata, K. Uchino and S. Nomura: Ferroelectrics **37** (1981) 579.
3) J. Kuwata, K. Uchino and S. Nomura: Jpn. J. Appl. Phys. **21** (1982) 1298.
4) T. Ogawa, Y. Yamauchi, Y. Numamoto, M. Matsushita and Y. Tachi: Jpn. J. Appl. Phys. **41** (2002) L55.
5) A.-É. Renault, H. Dammak, P. Gaucher, M. Pham Thi and G. Calvarin: Proc. 13th IEEE ISAF, Nara, Japan, 2002, p. 439.
6) In all the paper crystallographic directions and planes were indexed using the pseudo-cubic axes.
7) H. Dammak, A. Lebon and G. Calvarin: Ferroelectrics **235** (1999) 151.
8) A. Renault: Dr. Thesis, École Centrale de Paris, 2002.
9) A.-É. Renault, H. Dammak, G. Calvarin, M. Pham Thi and P. Gaucher: Jpn. J. Appl. Phys. **41** (2002) 3846.
10) Y. Uesu, M. Matsuda, Y. Yamada, K. Fujishiro, D. E. Cox, B. Noheda and G. Shirane: J. Phys. Soc. Jpn. **71** (2002) 960.
11) K. Nakamura and Y. Kawamura: IEEE Trans. Ultrason. Ferroelect. Freq. Control. **47** (2000) 750.
12) K. Nakamura, T. Tokiwa and Y. Kawamura: J. Appl. Phys. **91** (2002) 9272.
13) M. Zgonik, R. Schlesser, I. Baggio, E. Voit, J. Tscherry and P. Günter: J. Appl. Phys. **74** (1993) 1287.
14) K. Ohwada, K. Hiroya, P. W. Rehrig, P. M. Gehring, B. Noheda, Y. Fuji, S.-E. Park and G. Shirane: J. Phys. Soc. Jpn. **70** (2001) 2778.
15) S. Zhang, L. Laurent, S. Liu, S. Rhee, C. A. Randall and T. R. Shrout: Jpn. J. Appl. Phys. **41** (2002) L1099.
16) S. F. Liu, S. E. Park, T. R. Shrout and L. E. Cross: J. Appl. Phys. **85** (1999) 2810.
17) D. Berlincourt and H. Jaffe: Phys. Rev. **111** (1958) 143.
18) J. Yin and W. Cao: Ferroelctrics **251** (2001) 93.
19) D. Damjanovic, F. Brem and N. Setter: Appl. Phys. Lett. **80** (2002) 652.